JCB Article

The Rab8 GTPase selectively regulates AP-1B–dependent basolateral transport in polarized Madin-Darby canine kidney cells

Agnes Lee Ang, Heike Fölsch, Ulla-Maija Koivisto, Marc Pypaert, and Ira Mellman

Department of Cell Biology, Ludwig Institute for Cancer Research, Yale University School of Medicine, New Haven, CT 06520

The AP-1B clathrin adaptor complex plays a key role in the recognition and intracellular transport of many membrane proteins destined for the basolateral surface of epithelial cells. However, little is known about other components that act in conjunction with AP-1B. We found that the Rab8 GTPase is one such component. Expression of a constitutively activated GTP hydrolysis mutant selectively inhibited basolateral (but not apical) transport of newly synthesized membrane proteins. Moreover, the effects were limited to AP-1B–dependent basolateral cargo; basolateral transport of proteins containing dileucine targeting motifs that do not interact with AP-1B were targeted normally despite overexpression of mutant Rab8. Similar results were obtained for a dominant-negative allele of the Rho GTPase Cdc42, previously implicated in basolateral transport but now shown to be selective for the AP-1B pathway. Rab8-GFP was localized to membranes in the TGN-recycling endosome, together with AP-1B complexes and the closely related but ubiquitously expressed AP-1A complex. However, expression of active Rab8 caused a selective dissociation of AP-1B complexes, reflecting the specificity of Rab8 for AP-1B–dependent transport.

Introduction

Although epithelial cell polarity is initiated by spatial cues provided during cell–cell and cell–substrate contacts, the subsequent generation of biochemically distinct apical and basolateral plasma membrane domains is perhaps the most essential determinant of epithelial cell function (Drubin and Nelson, 1996; Mostov et al., 2000; Nelson, 2003). To a large extent, plasma membrane proteins are delivered to and maintained at the appropriate cell surface domain by distinct targeting signals that control polarized transport on the secretory and endocytic pathways (Mellman, 1996). This is best understood in the case of basolateral proteins, many of which possess distinctive tyrosine- or dileucine-containing sequence motifs in their cytoplasmic domains (Hunziker et al., 1991; Matter et al., 1992, 1994; Hunziker and Fumey, 1994; Matter and Mellman, 1994). Apical proteins are often selected for transport by interactions involving carbohydrate moieties in a protein's lumenal domain or by the lipid-binding properties of membrane anchors. Importantly, the same (or similar) sets of signals are decoded upon exit of newly synthesized proteins from the TGN and in endosomes for proteins internalized by endocytosis (Matter et al., 1993; Aroeti and Mostov, 1994; Odorizzi et al., 1996). The physiological importance of this recognition system has been demonstrated by human mutations causing familial hypercholesterolemia due to a defective targeting signal in the LDL receptor (LDLR; Koivisto et al., 2001).

Some of the components involved in basolateral transport have recently been identified. Among these is an epithelial cell–specific form of the AP-1 clathrin adaptor complex, AP-1B (Fölsch et al., 1999, 2003; Ohno et al., 1999). This tetrameric complex is closely related to the ubiquitously expressed AP-1A complex. The two differ only by substitution of the ubiquitous 50-kD μ1A subunit (AP-1A) with a homologous μ1B subunit (AP-1B), whose expression is limited to epithelia. The presence of μ1B confers the ability to recognize and mediate basolateral transport of membrane proteins bearing tyrosine-dependent targeting signals (e.g., LDLR, vesicular stomatitis virus G-protein [VSV-G], and asialoglycoprotein receptor) and at least one tyrosine-independent signal (transferrin [Tfn] receptor; Fölsch et al., 1999; Sugimoto et al., 2002). Interestingly, AP-1B does not program the basolateral targeting of proteins bearing dileucine-type

Address correspondence to Ira Mellman, Department of Cell Biology, Ludwig Institute for Cancer Research, Yale University School of Medicine, 333 Cedar St., PO Box 208002, New Haven, CT 06520-8002. Tel.: (203) 785-4303. Fax: (203) 785-4301. email: ira.mellman@yale.edu

Key words: Rab8; AP-1; sorting; polarity; MDCK

Abbreviations used in this paper: FcR, Fc receptor; IF, immunofluorescence; LDLR, LDL receptor; Tfn, transferrin; VSV-G, vesicular stomatitis virus G-protein.

signals (e.g., FcRII-B2), as these reach the basolateral surface of μ1B-negative LLC-PK1 cells (Roush et al., 1998; Fölsch et al., 1999). The precise site of AP-1B action is unknown, but it may act to control polarized sorting on both the endocytic and biosynthetic pathways, i.e., in endosomes and the TGN (Gan et al., 2002).

Clearly, other components must play a role in the formation and delivery of basolateral transport carriers. The Rho family GTPase Cdc42 has been found to play an essential role in basolateral targeting in MDCK cells (Kroschewski et al., 1999; Cohen et al., 2001; Musch et al., 2001), although it is unclear if this role is limited to AP-1B–dependent or –independent pathways. Similarly, the multi-subunit exocyst complex, first identified in yeast as being required for tethering secretory vesicles at the bud tip (TerBush et al., 1996), has also been implicated in basolateral transport. In MDCK cells, antibodies to two mammalian exocyst subunits (Sec6 and Sec8) partially inhibited the insertion of LDLR in the basolateral plasma membrane (Grindstaff et al., 1998; Yeaman et al., 2001; Moskalenko et al., 2002). Because LDLR has been identified as AP-1B–dependent cargo (Fölsch et al., 1999), it seems possible that the exocyst is involved in the AP-1B pathway.

The small GTPases that regulate exocyst function might therefore have a role in AP-1B–dependent sorting by supervising the organization of components required for sorting or vesicle delivery. In yeast, the Rab family member Sec4p is localized to transport vesicles and interacts genetically with the exocyst to facilitate the targeting of secretory vesicles to the plasma membrane (Guo et al., 1997, 1999). Rab8 is among the closest mammalian homologues to Sec4p and has, in fact, previously been associated with transport from the TGN to the plasma membrane in neurons and MDCK cells (Huber et al., 1993, 1995; Moritz et al., 2001). A role in basolateral transport was suggested by Rab8's association with basolateral vesicles upon cell fractionation, although the functional significance of this observation has remained unclear; only a slight inhibition of transport was seen in permeabilized MDCK cells using a peptide from the Rab8 hypervariable COOH-terminal domain (Huber et al., 1993).

Results

Activated Rab8 selectively affects basolateral transport

To better assess the role of Rab8 in polarized transport in epithelial cells, we adapted a microinjection assay for filter-grown MDCK cells previously used to illustrate the involvement of Cdc42 in basolateral targeting (Kroschewski et al., 1999). Cells were injected with cDNAs encoding ts045 VSV-G–GFP as a plasma membrane reporter together with constitutively active (Rab8Q67L, GTPase-deficient) or dominant-negative (Rab8T22N, nucleotide binding–deficient) forms of Rab8. Rab8 alleles contained an NH_2-terminal T7 tag to monitor expression (Peranen et al., 1996). Two forms of ts045 VSV-G–GFP were used, the first being the wild-type protein, an AP-1B–dependent basolateral marker (Fölsch et al., 2003), and the second being an apical variant (VSV-G–G3) bearing a cytoplasmic domain linker that appears to mask the AP-1B–binding site (Keller et al., 2001). After injection, the cells were incubated at the nonpermissive temperature for ts045 VSV-G, allowing it to accumulate in the ER while the expressed Rab8 accumulated in the cytosol. Subsequent transfer to the permissive temperature (31°C) in the presence of cycloheximide initiated synchronous transport of VSV-G through the Golgi and to the surface.

As shown in Fig. 1 A, expression of the constitutively active allele of Rab8 (Rab8Q67L) caused a great majority of VSV-G–GFP in any one cell to be expressed apically, in contrast to the lateral or basolateral expression obtained in cells injected with the dominant-negative Rab8 cDNA (Rab8T22N) or with the VSV-G–GFP cDNA alone. Overexpression of wild-type Rab8 elicited a phenotype similar to Rab8Q67L (unpublished data). In both cases, the effects were apparently selective for newly synthesized proteins and did not reflect an overall reorganization because the localization of the endogenous basolateral marker gp58 remained unchanged. Moreover, the expected apical localization of VSV-G–G3 variant was not affected (Fig. 1 B), suggesting that Rab8 activation selectively affected basolateral transport.

Although total cell fluorescence showed VSV-G–GFP mostly at the apical side of MDCK cells in the presence of activated Rab8, it was ambiguous whether VSV-G had accumulated in vesicles near the cell apex or at the apical surface. To distinguish these possibilities, we assayed surface appearance using an antibody against the ectodomain of VSV-G (generated by the late Thomas Kreis, and thus designated TK-G) on nonpermeabilized cells. As shown in Fig. 1 C, VSV-G was clearly detected at the apical surface in the Rab8Q67L-expressing cells; basolateral VSV-G was only detected in cells not injected with Rab8 (Fig. 1 C) or with the dominant-negative allele (unpublished data). Thus, expression of active Rab8 caused the missorting of VSV-G to the apical plasma membrane. This phenotype was obtained in >80% of the cells judged to be coexpressing VSV-G and Rab8Q67L (Rab8-expressing cells were visualized using an antibody to T7 as in Fig. 1 B).

Rab8Q67L expression may have caused ectopic expression of VSV-G, but it also might have had an effect on the overall efficiency of VSV-G transport, a feature that might have been missed by fluorescence microscopy alone. Therefore, we performed FACS® analysis on nonpermeabilized cells to compare the efficiency of VSV-G surface arrival in the presence or absence of activated Rab8, using the TK-G antibody. To ensure that a substantial population of cells expressed VSV-G with or without Rab8, MDCK cells were infected with recombinant adenoviruses encoding the VSV-G–GFP and Rab8Q67L genes described above. The FACS® analysis revealed that the level of cell surface VSV-G expression was unchanged by activated Rab8 expression (Fig. 1 D), indicating that Rab8Q67L does not inhibit the delivery of VSV-G to the plasma membrane. Although only ~50% of the cells in the population expressed both markers, we noted no decrease in the level of TK-G binding. Together, these data suggested that Rab8 has a selective role in the sorting or targeting of basolaterally directed cargo, and that expression of Rab8Q67L does not cause overall defects in polarity or the secretory pathway.

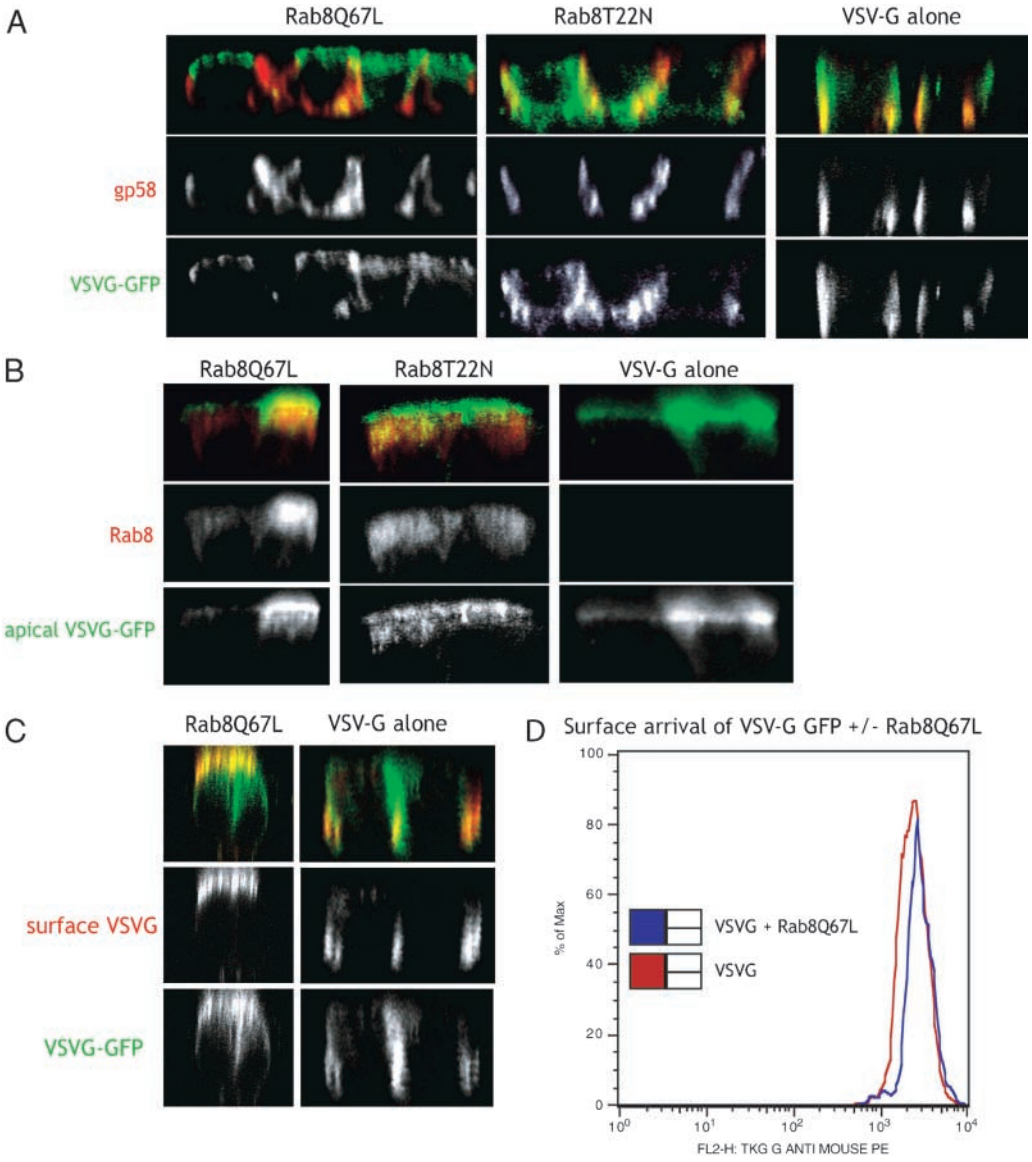

Figure 1. **Activated Rab8 (but not dominant-negative Rab8) mislocalizes VSV-G to the apical surface.** (A) Fully polarized MDCK cells were microinjected with cDNAs of ts045 VSV-G GFP and T7-tagged Rab8Q67L (dominant active) or Rab8T22N (dominant negative) at 200 ng/μl, incubated at the nonpermissive temperature of 40°C to accumulate VSV-G in the ER for 2 h, and chased for 2 h at the permissive temperature of 31°C in the presence of cycloheximide. The cells were fixed, permeabilized, and processed for IF. Indirect IF of an endogenous basolateral protein using the anti-gp58 antibody (red, second row), followed by Alexa® 568 secondary antibody. The cells were analyzed by confocal microscopy and a representative x-z section is shown. (B) Polarized MDCK cells were microinjected with the cDNAs of apical ts045 VSV-G–G3 with T7-Rab8Q67L or T7-Rab8T22N under the same pulse-chase conditions as above. Cells were processed for IF as above. Rab8 expression (red, second row) was monitored using a mouse anti-T7 tag antibody followed by anti–mouse Alexa® 568 secondary antibody. (C) ts045 VSV-G–GFP was microinjected with T7-Rab8Q67L under the same pulse-chase conditions as in A, but the chase is followed by fixation without permeabilization. The cells are immunolabeled using an antibody, TK-G, against the ectodomain of VSV-G followed by Alexa® 568 secondary antibody. (D) Confluent MDCK cells were infected overnight at 40°C with adenoviruses encoding ts045 VSV-G–GFP and T7-Rab8Q67L. After a 2-h chase at 31°C in the presence of cycloheximide, the cells were trypsinized, fixed without permeabilization, and immunolabeled using the TK-G antibody followed by an anti–mouse phytoerythrin secondary antibody. FACS® analysis shows that the efficiency of surface expression of VSV-G is unchanged in the presence of Rab8Q67L.

Newly synthesized VSV-G is directly missorted to the apical surface in cells expressing activated Rab8

We sought to determine if activated Rab8 acted to directly missort newly synthesized VSV-G on the secretory pathway or indirectly after initial basolateral insertion and missorting during endocytosis and recycling. For this purpose, filter-grown MDCK cells were doubly infected with adenoviruses encoding ts045 VSV-G–GFP or activated Rab8, and the surface appearance of VSV-G was analyzed by pulse-chase radiolabeling and surface biotinylation. As expected, in the absence of exogenous Rab8 expression, VSV-G appeared at the basolateral surface, reaching a plateau within 60–90 min and decreasing (in some experiments) thereafter (Fig. 2). Importantly, little VSV-G was detected at the apical surface at early or late times of chase. However, in cells coinfected with activated Rab8, VSV-G appeared simultaneously at

both the apical and basolateral surfaces at times as early as 30 min of chase. The delivery of VSV-G to the apical surface without prior appearance at the basolateral surface strongly suggested that missorting occurred on the secretory pathway upon exit from the TGN rather than in endosomes after endocytosis from the basolateral domain.

Relative to the immunofluorescence (IF) results (Fig. 1), a significant fraction of VSV-G was, however, delivered to the basolateral surface in these experiments. This almost certainly reflected the fact that under the conditions of dual adenovirus infection used here (as opposed to microinjection), only 50% of the cells expressing VSV-G also expressed Rab8. Thus, the observed effect of apical VSV-G expression caused by Rab8 activation would be underestimated due to the absence of Rab8 expression in half the cells expressing VSV-G.

Expression of mutant Rab8 missorts only AP-1B cargo

To determine whether Rab8 caused the missorting of all basolateral proteins regardless of their specific targeting determinants, we analyzed basolateral reporters that have been shown to be AP-1B–dependent or –independent using the microinjection assay. The immunoglobulin Fc receptor (FcR) relies on a dileucine motif for localization (Matter et al., 1994) and was found to reach the basolateral surface of polarized pig kidney epithelial (LLC-PK1) cells even in the absence of μ1B expression (Roush et al., 1998; Fölsch et al., 1999). LDLR, on other hand, depends on tyrosine motifs for basolateral sorting (Matter et al., 1992) that physically interact with AP-1B adaptors and require μ1B expression for basolateral targeting in LLC-PK1 cells (Ohno et al., 1998; Fölsch et al., 1999, 2001; Sugimoto et al., 2002). For these experiments, a Rab8-GFP was used to monitor expression while surface polarity of FcR and LDLR was detected by staining nonpermeabilized cells with antibodies to the ectodomain of each receptor.

It was necessary to alter the temperature shift protocol used earlier in order to accommodate reporter proteins that, unlike ts045 VSV-G, could not be accumulated in the ER at 40°C before assay. Thus, after microinjection, cells were maintained at 20°C for 2.5 h to accumulate each reporter (i.e., FcR and LDLR) in the TGN before release by shifting the temperature up to 31°C. As a control, we first established that this protocol resulted still in the missorting of ts045 VSV-G in mutant Rab8-expressing cells (unpublished data). After microinjection of wild-type or mutant Rab8-GFP together with LDLR or FcR cDNAs, the receptors were accumulated in the Golgi complex by incubation at

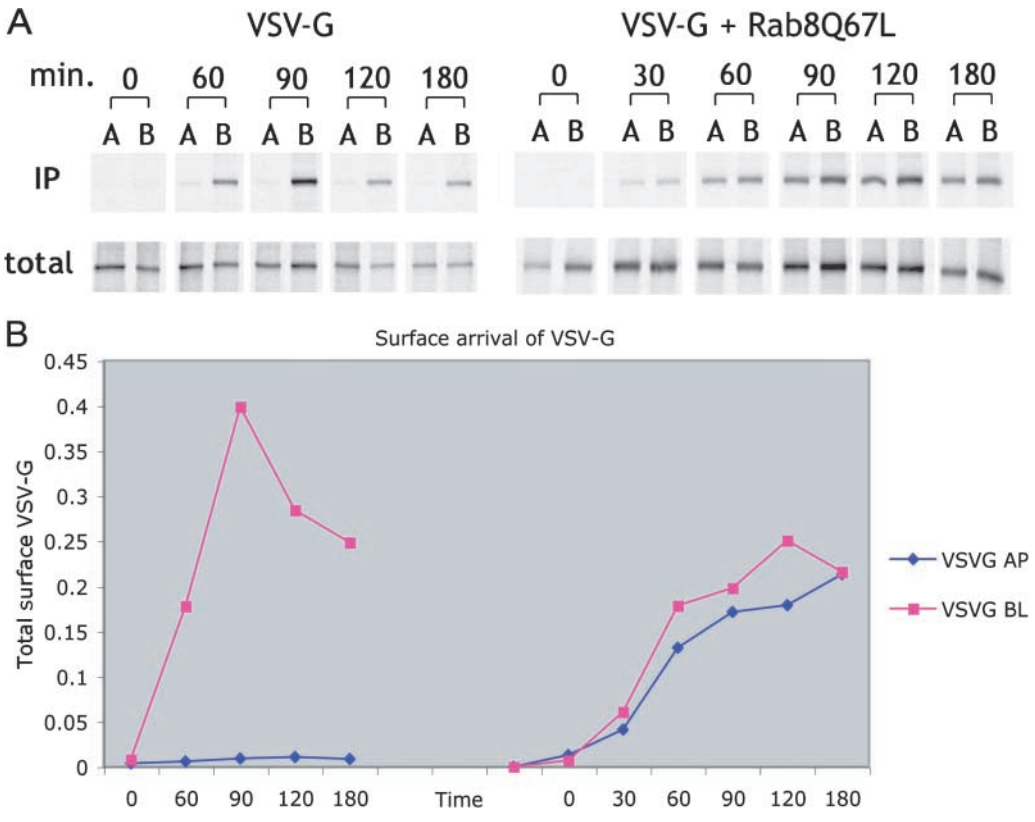

Figure 2. **Activated Rab8 causes the missorting of VSV-G to the apical surface in the biosynthetic pathway.** (A) Polarized MDCK cells were infected overnight with VSV-G–GFP and Rab8Q67L adenoviruses and pulse-labeled with [^{35}S]Met/Cys for 15 min. Cells were then incubated at 37°C in medium containing fivefold excess methionine and cysteine for the indicated times. After the chase, cells were placed in ice-cold PBS^{++} and biotinylated on either the apical (A) or basolateral (B) surfaces. VSV-G was immunoprecipitated using the P5D4 antibody, and the antibody complexes were pulled down with protein G–Sepharose. After spinning down the beads, 20% of the immunoprecipitated protein was set aside as the "total," whereas the remaining 80% was applied to neutravidin beads in order to isolate the biotinylated membranes. All samples were run on 10% SDS-PAGE gels. The gels were dried and quantitative autoradiography was performed. (B) Graphical representation of the quantitation of the signal of total VSV-G at the surface in the absence or presence of activated Rab8 from A. VSV-G at the apical (AP) surface is in blue and VSV-G at the basolateral (BL) side is in red.

20°C (2.5 h) followed by release at 37°C in the presence of cycloheximide. As found for VSV-G, which also uses an AP-1B–dependent tyrosine-based sorting motif (Thomas and Roth, 1994; Fölsch et al., 2003), LDLR was missorted to the apical surface in the presence of activated Rab8 (Fig. 3 A). In striking contrast was the behavior of FcR. As shown in Fig. 3 B, FcR remained at the basolateral surface despite the efficient expression of the active Rab8 mutant Rab8Q67L. Identical results for both receptors were obtained using non-GFP-tagged Rab8 (unpublished data). Thus, it appeared that mutant Rab8 expression affected only the polarity of AP-1B–dependent cargo.

To demonstrate that the regulation by Rab8 was due to the active, membrane-bound allele, cDNA encoding a nonprenylated GFP-tagged activated Rab8 (Rab8ΔC) was microinjected with LDLR cDNA and analyzed for LDLR surface expression. As shown in Fig. 3 A, expression of the nonprenylated activated Rab8 had no effect on LDLR surface localization, suggesting that proper membrane localization of Rab8 is important for regulating the basolateral pathway.

In a further control for the specificity of Rab8's effect, we microinjected wild-type or mutant GFP-tagged Rab11, a GTPase that has an intracellular distribution similar to that of Rab8 (Fig. 3 A) and that is also a structural relative of Rab8 and Sec4p. However, unlike Rab8Q67L, activated Rab11 (Rab11Q70L) had no effect on LDLR transport to the basolateral plasma membrane (Fig. 3 A). Thus, whatever its mechanism, the phenotype of missorting tyrosine motif–containing basolateral proteins was specific to active Rab8, and not a general consequence of disrupting the function of Rab family proteins in the recycling endosome/TGN region of the cytoplasm.

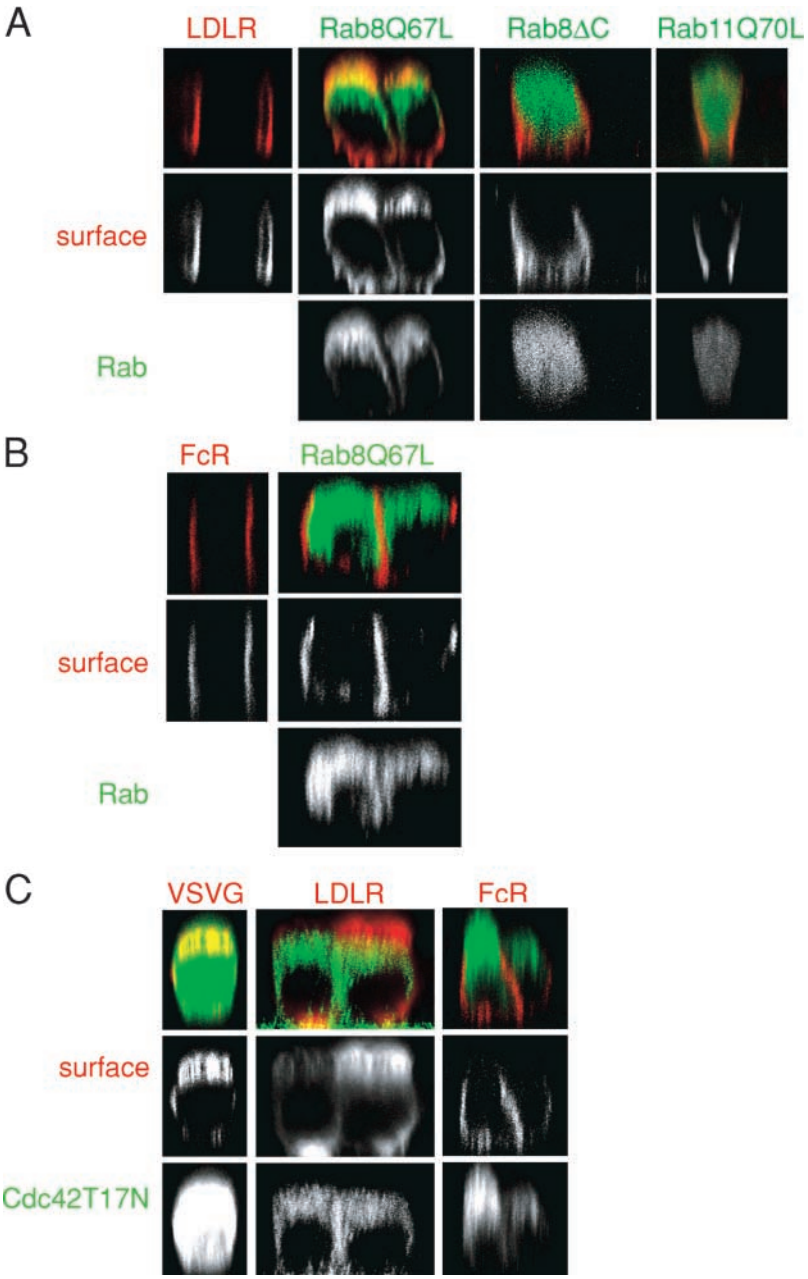

Figure 3. **Activated Rab8 missorts only AP-1B cargo.** (A–C) Fully polarized MDCK cells were microinjected with the cDNAs encoding activated GFP-Rab8 (Rab8Q67L; A, second column), nonprenylated GFP-Rab8 (Rab8ΔC; A, third column), activated GFP-Rab11 (Rab11Q70L; A, fourth column), or dominant-negative GFP-Cdc42 (Cdc42T17N) (C) with LDLR (A and C, red) or FcR (B and C, red). After injection, the cells were incubated at 37°C for 1 h, at 20°C for 2.5 h, and finally at 37°C for 2 h in the presence of cycloheximide. Cells were fixed without permeabilization and stained for surface LDLR (C7) or FcR (24G2), followed with Alexa® 568 secondary antibodies. GTPases are visualized by GFP fluorescence. Images are representative confocal z-sections.

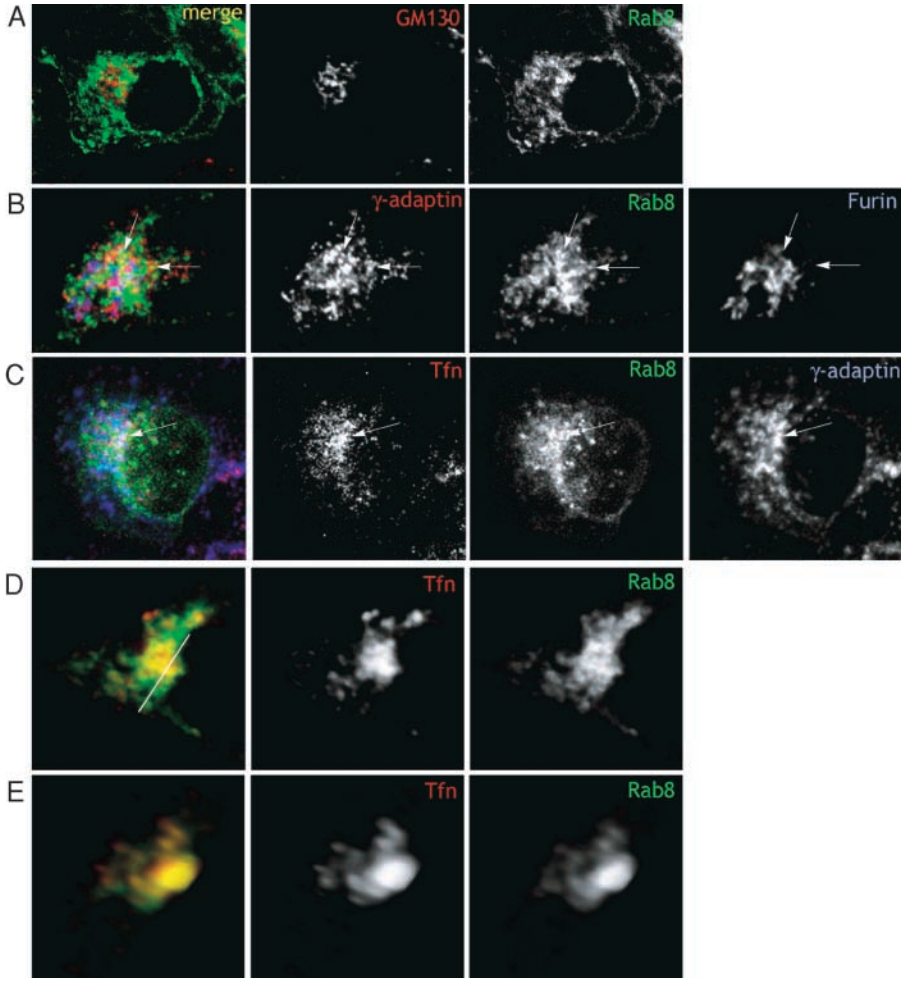

Figure 4. **Rab8 is localized to the perinuclear region, associating with recycling endosomes.** (A and B) MDCKT (stably transfected with cDNA for Tfn receptor) cells grown on coverslips were microinjected with 50 ng/μl wild-type GFP-Rab8 and were incubated at 37°C for 2 h. Cells were processed for IF and stained for the Golgi (A; GM130, red) and the TGN (B; γ-adaptin [red] arrows indicate colocalization of γ-adaptin with Rab8, and absence of colocalization with furin [blue]). (C) MDCKT cells were induced for 14 h with butyrate to express Tfn receptor, then microinjected with cDNA for 50 ng/μl wild-type GFP-Rab8 and incubated at 37°C for 2 h. After cold-binding Alexa® 594–Tfn, cells were incubated for 22 min at 37°C to accumulate Tfn in recycling endosomes. Colocalization of Tfn, Rab8, and γ-adaptin (arrow). Tfn, red; Rab8, green; γ-adaptin, blue. (D) Three-dimensional reconstruction of confocal serial sections, x-y plane of a representative cell as in C. (E) Same cell from D cut sagittally (white line in first panel of D) and rotated ~45° to view colocalization of Tfn with Rab8.

Expression of mutant Cdc42 also missorts only AP-1B cargo

In previous work, we found that expression of mutant Cdc42, especially a Cdc42 dominant-negative allele, caused the missorting of basolateral but not apical cargo (Kroschewski et al., 1999), a finding confirmed by others (Johnson, 1999; Joberty et al., 2000; Cohen et al., 2001; Musch et al., 2001). Because this effect was observed for VSV-G, we next asked if Cdc42 might also selectively regulate the AP-1B–sorting pathway. For these experiments, we again used the 20°C temperature shift protocol to allow the use of LDLR and FcR as reporters in addition to VSV-G. As shown previously, when Cdc42 was functionally deleted by microinjection of a cDNA encoding a dominant-negative allele (Cdc42T17N), VSV-G was missorted to the apical surface of filter-grown MDCK cells (Fig. 3 C). Similar results were obtained when the polarized expression of a second AP-1B cargo protein LDLR was monitored (Fig. 3 C). However, dominant-negative Cdc42 caused no detectable alteration in the basolateral expression of FcR, an AP-1B–independent basolateral protein (Fig. 3 C). Together, these observations strongly suggested that expression of Rab8 and dominant-negative Cdc42 selectively affected the localization of basolateral proteins that rely on AP-1B adaptor. Even though the precise mechanism by which either GTPase elicits its effects is not yet clear, it does seem that they are restricted to a common basolateral-sorting pathway.

Rab8 is localized to the perinuclear region in recycling endosomes

To understand the role of Rab8 in the AP-1B–dependent basolateral sorting pathway, we examined the localization of Rab8 in MDCK cells. Although previous work had localized Rab8 to the "Golgi region" (Huber et al., 1993; Peranen et al., 1996; Peranen and Furuhjelm, 2001), its distribution remains unclear. cDNAs encoding GFP-tagged Rab8, wild type, or Rab8Q67L were microinjected at low concentration (to provide trace labeling) into MDCK cells grown on coverslips. After fixation, the cells were colabeled with antibodies against various compartments, particularly the TGN and recycling endosomes, thought to be sites of polarized sorting. As shown in Fig. 4, wild-type Rab8 was localized to the perinuclear region, although in some cells labeling was occasionally in peripheral structures as well as possibly on plasma membrane. However, the perinuclear Rab8-GFP was excluded from structures positive for GM130, a cis-Golgi marker (Fig. 4 A), as well as for giantin, a pan-Golgi marker (unpublished data), indicating that this portion of its distribution did not reflect an association with Golgi cisternae. Similar results were obtained for Rab8Q67L-GFP (unpublished data).

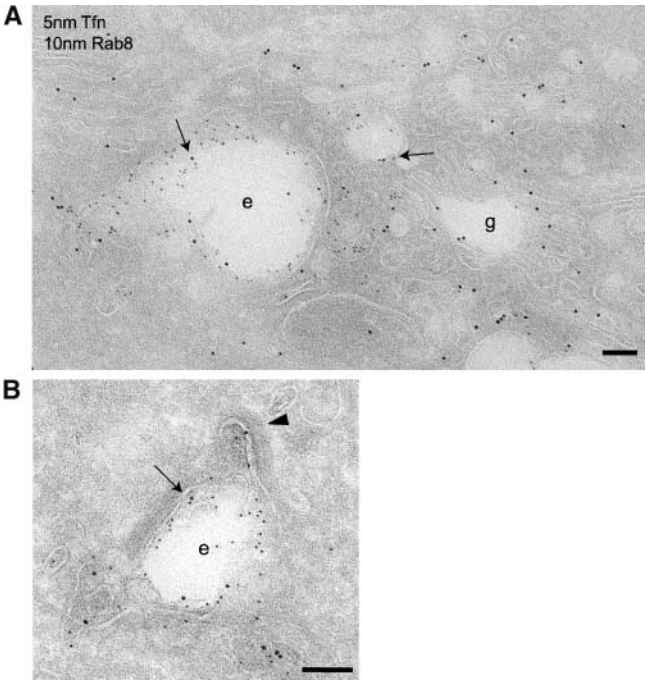

Figure 5. **Rab8 colocalizes with Tfn in recycling endosomes.** (A and B) Rab8 (10-nm gold) and Tfn (5-nm gold) are localized on endosomes (arrows) and vesicle bud (arrowhead) in MDCKT cells infected with GFP-Rab8 adenovirus. GFP-Rab8 and Alexa® 488-Tfn were visualized using anti-GFP and anti-Alexa® 488 antibodies, respectively, followed by IgG secondary antibodies and protein A–gold. e, endosome; g, Golgi. Bar, 100 nm.

A closer spatial relationship was observed between Rab8-GFP and the AP-1 adaptor subunit γ-adaptin, although the frequency of actual colocalizing structures was very low (Fig. 4 B, arrows). This result was difficult to interpret because MDCK cells express two γ-adaptin–containing complexes, AP-1A and AP-1B. Because the two complexes may have distinct distributions (Meyer et al., 2000), a preferential localization of Rab8 with AP-1B might be obscured. However, no colocalization was observed between Rab8-GFP and furin, an endogenous membrane protein that recycles between the TGN and endosomes as AP-1A–dependent cargo (Fig. 4 B; Teuchert et al., 1999). Conceivably, the slight codistribution between Rab8-GFP and γ-adaptin reflected a selective association of Rab8 with AP-1B (see Fig. 6).

At least a fraction of Rab8 appeared to associate with recycling endosomes, evidenced by the partial colocalization of GFP-Rab8 with internalized Tfn (Sheff et al., 1999; Fig. 4 C, arrow). This coregional distribution was particularly evident in cells where the recycling endosomes were characteristically clustered in the perinuclear cytoplasm, although markers of cisternal Golgi and the TGN continued to be distinct from Rab8-GFP (unpublished data). Three-dimensional reconstruction of z-axis sections was used to further evaluate the spatial relationship of Rab8-GFP and Tfn (Fig. 4 D). Upon rotating such images and sectioning them sagittally (Fig. 4 E), it was apparent that in areas of coregionalization, the overlap between Rab8-GFP and Tfn was found throughout the volume of the structures observed (Fig. 4, D and E, yellow). Thus, the areas of overlap did not represent separate structures superimposed across different focal planes. To provide more direct evidence, immuno-EM was performed on cells prepared as in Fig. 4 D. As shown in Fig. 5 (A and B), at least a fraction of Rab8 (10-nm gold) was clearly localized to the Tfn-positive (5-nm gold) endosomes (arrows) and coated vesicle buds (arrowhead). As expected from the IF data, some Rab8 labeling was also found associated with Golgi elements. In any event, the EM data suggest that recycling endosomes may be the site of action of Rab8, and thus a possible site for sorting of AP-1B–specific cargo.

Activated Rab8 interferes with the localization of γ-adaptin

Because Rab8 was localized to the same vicinity as γ-adaptin and selectively disrupted the basolateral transport of AP-1B–dependent cargo, we next determined if overexpression of activated Rab8 might also disrupt the distribution of AP-1B complexes. Coverslip-grown MDCK cells were injected with a high concentration of activated Rab8 cDNA (to induce relative overexpression) and labeled for Rab8 and various Golgi or TGN markers. Although expression of activated Rab8 had no effect on the localization of Golgi- or TGN-resident proteins, Fig. 6 A illustrates that it did alter the distribution of γ-adaptin from a relatively compact perinuclear cluster to one that is more diffuse (top panels, arrows; arrowheads show γ-adaptin in three noninjected cells). As a control, we also expressed a nonprenylated Rab8 mutant (Rab8ΔC) under the same conditions; there was no detectable effect on γ-adaptin localization (Fig. 6 A, bottom panels; arrowheads). The distribution of TGN and cisternal Golgi residents, furin and giantin (respectively), was not affected by activated Rab8 overexpression (Fig. 6 B), suggesting that only γ-adaptin–containing membranes or γ-adaptin membrane association were subject to disruption by Rab8.

Activated Rab8 disrupts γ-adaptin on AP-1B complexes

γ-adaptin is present in both AP-1A and -1B complexes. Because active Rab8 expression might only interfere with AP-1B, we next sought to determine if Rab8's effects were manifested selectively. For this purpose, we took advantage of two cell lines, the porcine kidney epithelial cell line LLC-PK1 that is deficient in μ1B expression, and fibroblast cells isolated from a μ1A knockout mouse that had been stably transfected with μ1B (Fölsch et al., 1999; Zizioli et al., 1999; Meyer et al., 2000; Eskelinen et al., 2002). Thus, we could analyze cells with all three phenotypic combinations of μ1A and μ1B.

As shown in Fig. 7 A (top panels), expression of Rab8Q67L in AP-1A+/AP-1B− LLC-PK1 cells did not cause the dispersal of γ-adaptin seen in MDCK cells (which are AP-1A+/AP-1B+). Thus, it appeared that Rab8 activation had no effect on AP-1A adaptor localization or membrane recruitment. γ-Adaptin staining remained similar to that of the AP-1A cargo protein TGN-38 (expressed from a cotransfected cDNA; Fig. 7 A, blue). In contrast, the localization of γ-adaptin was substantially altered in LLC-PK1 cells that had been transfected with a μ1B cDNA and thus expressed functional AP-1B (Fig. 7 A, bottom, AP-1A+/AP-1B+). Notably, some γ-adaptin staining did persist in

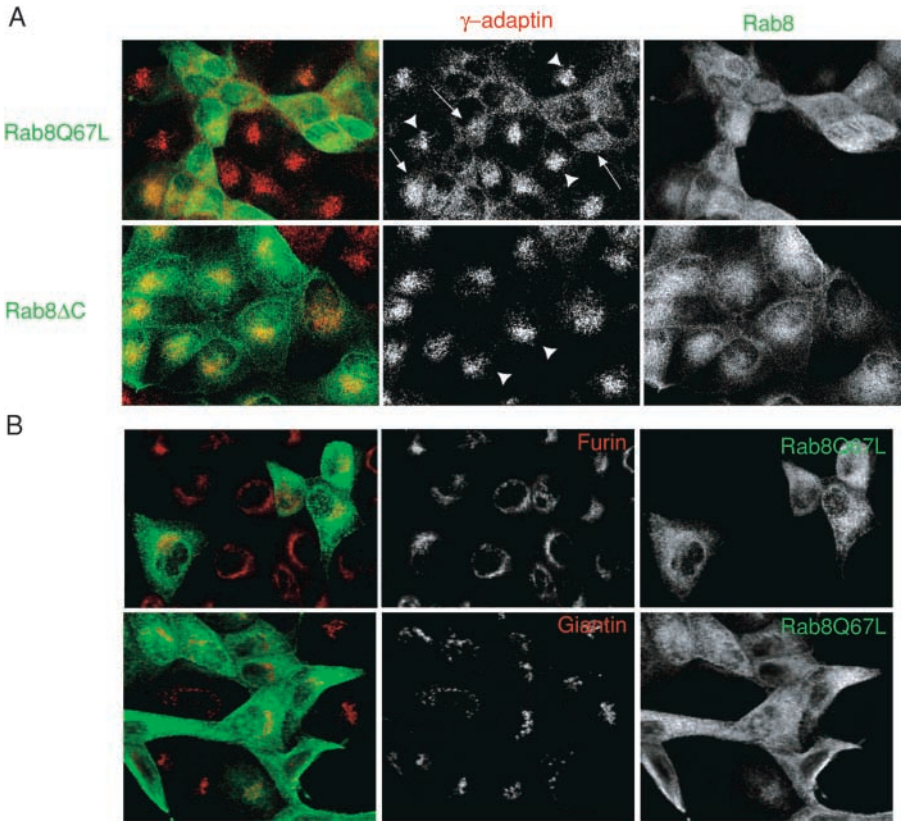

Figure 6. **Activated Rab8 disrupts γ-adaptin localization in MDCK cells, but does not disrupt Golgi- or furin-containing regions of the TGN.** (A) Top: MDCK cells grown on coverslips were microinjected with the cDNA for T7-Rab8Q67L (200 ng/μl), incubated at 37°C for 2 h, fixed, permeabilized, and stained with anti-γ-adaptin antibody 100/3 (red, second column) or anti-T7 (green, third column). Arrows, cells expressing Rab8Q67L where γ-adaptin localization is disrupted; arrowheads, cells not expressing Rab8 with normal γ-adaptin localization. Bottom: cells were injected with cDNA for nonprenylated, activated GFP-Rab8ΔC (green, third column). Arrowheads, cells expressing Rab8ΔC have normal γ-adaptin localization (red, second column). (B) MDCK cells were microinjected with cDNA of T7-Rab8Q67L, incubated at 37°C for 2 h, and processed for IF with the TGN antibody anti-furin (A; top, second column), for the Golgi with anti-giantin (B; bottom, second column), and for T7-Rab8 (A and B, third column).

the perinuclear region of AP-1B–expressing LLC-PK1 cells. These structures most likely reflected the γ-adaptin subunits of AP-1A adaptor complexes, as their staining pattern was similar to TGN-38.

We quantified (double-blinded) the number of cells exhibiting γ-adaptin disruption in both AP-1A+/AP-1B− and AP-1A+/AP-1B+ LLC-PK1 cells. As summarized in Table I, activated Rab8 caused the dispersal or mislocalization of γ-adaptin in 60% of the AP-1B–expressing LLC-PK1 cells. Literally none of the wild-type LLC-PK1 cells was judged to exhibit a clear disruption in γ-adaptin localization in the presence of activated Rab8. In each case, approximately one quarter of the transfected cells exhibited an ambiguous phenotype.

Finally, we examined the phenotype of γ-adaptin localization as a function of activated Rab8 expression in the murine AP-1A−/AP-1B+ cells. Given that μ1A expression causes early embryonic lethality and that μ1B only incompletely substitutes for μ1A even in cell culture (Meyer et al., 2000; Fölsch et al., 2001; Eskelinen et al., 2002), it was not surprising to find that these cells were somewhat pleiomorphic in shape. Nevertheless, expression of active Rab8-GFP induced a disruption of the perinuclear γ-adaptin (AP-1B) staining pattern (Fig. 7 B, top panels; arrowheads denote γ-adaptin in untransfected cells). Instead of being characteristically clustered at one side of the nucleus, γ-adaptin appeared more diffuse, and as a result, less intensely stained. Control experiments (transfection of a GFP vector alone) did not alter the γ-adaptin staining pattern (Fig. 7 B, bottom panels). Quantitation was again performed, revealing that nearly 80% of the knockout cells containing AP-1B alone exhibited a dispersal of γ-adaptin upon Rab8Q67L expression (Table I). Less than 10% of those cells exhibited γ-adaptin disruption when GFP vector alone was expressed. These data strongly suggested that activated Rab8 disrupted only AP-1B complexes because γ-adaptin was mislocalized only in those

Table I. **Percentage of cells exhibiting dispersed γ-adaptin following expression of activated Rab8Q67L**

Cell type	AP-1 phenotype	Rab8 expressed	TGN organization (percentage of transfected cells)		
			Dispersed	Not dispersed	Other
LLC-PK1	AP-1A+/AP-1B−	Rab8Q67L	0	76	25
	AP-1A+/AP-1B+	Rab8Q67L	60	14	23
EFA	AP-1A−/AP-1B+	GFP alone	7	93	ND
	AP-1A−/AP-1B+	GFP-Rab8Q67L	79	18	ND

The numbers of cells with TGN disruption were counted in cells of each genotype, AP-1A only (AP-1A+/AP-1B−), AP-1A+/AP-1B+, and AP-1B only (AP-1A−/AP-1B+) in the presence of GFP-Rab8Q67L or GFP vector alone. The SEM for Rab8Q67L expressed in LLC-PK1 AP-1A+/AP-1B− and AP-1A+/AP-1B+ was 13 and 20%, respectively. The SEM for the EFA cells expressing GFP alone or GFP-Rab8Q67L was 12 and 15%, respectively. The SEM was calculated as the square root of n (n = number of cells). EFA, embryonic fibroblast cells; ND, not determined.

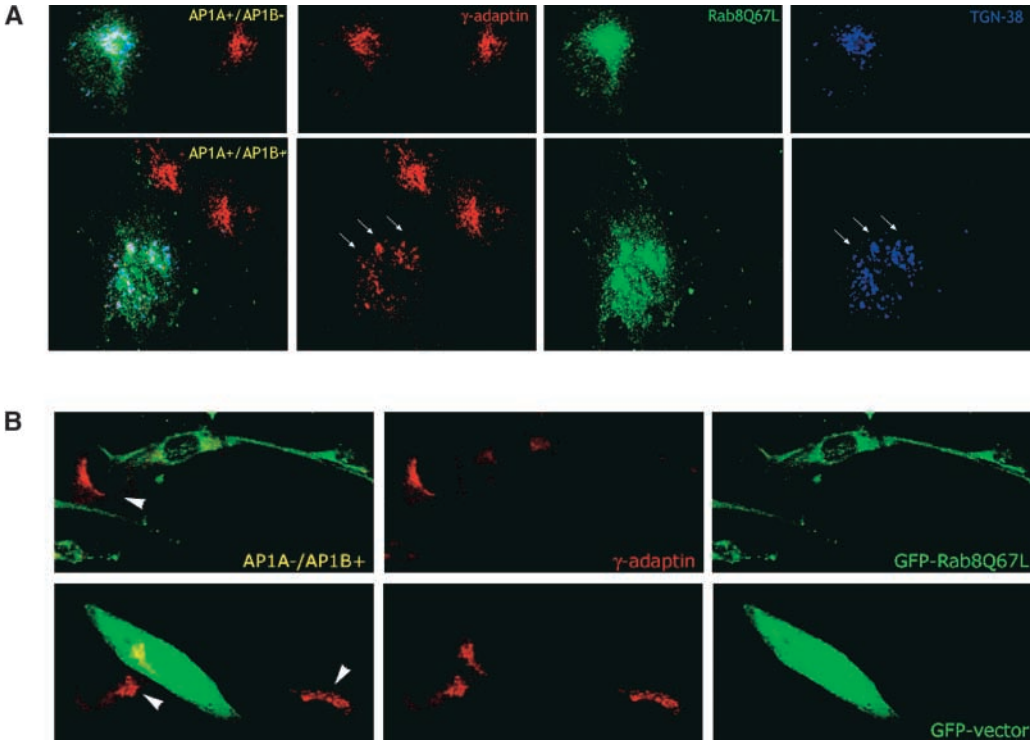

Figure 7. **Activated Rab8 causes the selective disruption of AP-1B complexes.** (A) LLC-PK1 cells were transfected with cDNAs for GFP-Rab8Q67L and TGN-38, and then were processed for IF with γ-adaptin 100/3 (red, second column) and TGN-38 using anti-TGN-38 antibody (blue, fourth column). Top, wild-type LLC-PK1 cells (AP-1A+/AP-1B−); bottom, LLC-PK1 stably transfected with μ1B gene (AP-1A+/AP-1B+). Arrows, colocalization of γ-adaptin with TGN-38. Notice there is no change in γ-adaptin localization in cells that express only AP-1A (top) even in the presence of Rab8Q67L expression. (B) Embryonic fibroblast cells expressing only AP-1B (AP-1A−/AP-1B+) were transfected as above with cDNA for GFP-Rab8Q67L or GFP vector alone (green). Mouse anti-γ-adaptin antibody clone 88 (red). Arrowheads, nontransfected cells with normal γ-adaptin localization.

cells expressing μ1B. Thus, Rab8 may directly or indirectly regulate the assembly or function of AP-1B complexes.

Discussion

Although the AP-1B complex plays an essential role in at least a subset of basolateral-targeting events in vertebrate epithelia, there are many questions as to its mechanism of action. For example, the site (or sites) at which AP-1B acts remains unclear. It is reasonable to presume that AP-1B controls sorting of newly synthesized membrane proteins upon exit from the TGN. However, it is unknown if sorting occurs at the level of the TGN or at some post-TGN site (e.g., recycling endosomes). There is also evidence that AP-1B acts in addition, possibly even preferentially in endosomal compartments, to mediate basolateral sorting after endocytosis (Gan et al., 2002).

Understanding the pathway controlled by AP-1B will be facilitated by identifying and characterizing the protein components with which it must collaborate. We have identified two such components, Rab8 and Cdc42. Rab8 had early on been implicated in basolateral transport in MDCK cells. This suggestion came from work demonstrating a partial inhibition of VSV-G insertion into the basolateral plasma membrane of permeabilized cells treated with a Rab8 hypervariable domain peptide (Huber et al., 1993). However, anti-Rab8 antibodies were without effect. Moreover, it remained unclear if the peptide's effect applied to all forms of basolateral transport or was selective for the AP-1B pathway (which had not yet been identified). Similarly, although Cdc42 had also been shown to be involved in basolateral transport, until now there was no indication that its effects were selective for the AP-1B pathway. The high degree of specificity exhibited by both Rab8 and Cdc42 for inhibiting AP-1B–dependent cargo strongly suggests that they functionally interact, even if indirectly, with the AP-1B complex, and that they help define a common pathway.

As a homologue of yeast Sec4p, it seems likely that Rab8 might also function together with the mammalian exocyst complex. Although we have not demonstrated such an interaction directly, it is important to note that at least two exocyst components (Sec6 and Sec8) have been associated with the delivery of AP-1B cargo (e.g., LDLR) to the basolateral surface of MDCK cells (Grindstaff et al., 1998). Moreover, expression of μ1B in LLC-PK1 cells enhances the recruitment of exocyst subunits (Sec8 and Exo70) to the TGN/recycling endosome region of AP-1B–negative LLC-PK1 cells (Fölsch et al., 2003). Rab8, too, was found in the same region.

Our findings have one further implication for understanding polarized transport in MDCK cells. They clearly indicate that there are two distinct modes of reaching the basolateral plasma membrane. In LLC-PK1 cells (which do not express μ1B), dileucine-containing membrane proteins such as FcR are nevertheless targeted basolaterally, suggesting

the existence of a second, AP-1B–independent pathway or mechanism of sorting in these cells. The fact that in μ1B-positive MDCK cells, expression of mutant Rab8 and Cdc42 had no effect on FcR polarity suggests that a similar mechanism was simultaneously operative despite the presence of AP-1B adaptors. Although this result suggests that the AP-1B–independent pathway reflects the formation of a distinct class of transport carriers, it remains possible that the dileucine-specific adaptor recruits its cargo to the same carriers as does AP-1B. Such a mechanism would be similar to what has recently been proposed for the selection of GGA and AP-1A cargo into clathrin-coated buds at the TGN during transport to lysosomes in mammalian cells (Hirst et al., 2000; Puertollano et al., 2001). However, it is unlikely that the AP-1B–independent pathway in MDCK cells (or LLC-PK1 cells) reflects the mechanism of basolateral targeting in polarized cells such as hepatocytes or neurons. Such cells do not express μ1B, yet they mediate the basolateral (or somato-dendritic) delivery of membrane proteins in a fashion strictly dependent on AP-1B signals (Jareb and Banker, 1998; Koivisto et al., 2001). Similarly, in *Drosophila* eye disc epithelial cells, which do not express a second μ1 gene, mammalian AP-1B–dependent cargo is nevertheless targeted accurately to the basolateral surface again in a signal-dependent fashion (unpublished data).

How and where does Rab8 work? The fact that Rab8-GFP was localized to the perinuclear region of MDCK cells, as suggested previously for endogenous Rab8 (Huber et al., 1993), suggests that it exerts at least part of its function during sorting or vesicle formation. Indeed, expression of active Rab8 was found to cause missorting of newly synthesized VSV-G to the apical surface. It also caused a selective disruption of AP-1B's association with membranes in the perinuclear region; remarkably, AP-1A's association with membranes in the same region was not affected by active Rab8 expression. Because there are now clear examples (e.g., Rab9) of Rab proteins playing an accessory role in sorting or transport vesicle formation (Carroll et al., 2001), such a function for Rab8 is indeed plausible. This is not inconsistent with early findings that Rab8 can be found on immunoisolated basolateral transport vesicles (Huber et al., 1993), or that it might also work (by analogy to Sec4p) in an exocyst-mediated tethering event before fusion at the basolateral membrane.

Similar considerations apply to Cdc42. It is found in the Golgi region of MDCK cells (Erickson et al., 1996) and has also been associated with more rapid export of basolateral cargo from the perinuclear zone (Musch et al., 2001). However, Cdc42 may interact with exocyst components and also is found in a ternary complex together with Par3, Par6, and PKDμ at junctional complexes in MDCK cells (Joberty et al., 2000; Zhang et al., 2001), all suggesting a possible role in plasma membrane tethering or fusion.

Our confocal microscopy results suggest that despite the close spatial apposition of Rab8-GFP to AP-1B adaptors and recycling endosomes, the actual degree of "overlap" is limited. Based on our EM data, it would appear that Rab8 localizes extensively with Tfn-containing recycling endosomes. Indeed, Sec8 and Exo70 also appear to exhibit a similar recycling endosome-like pattern in AP-1B–expressing cells (Fölsch et al., 2003). Such observations suggest that polarized sorting may actually occur after exit of AP-1B cargo from the TGN, perhaps in recycling endosomes or a subcompartment closely apposed to these sites. A functional relationship between the TGN and recycling endosome has long been suspected. The finding that a Rab protein controlling the transport of newly synthesized plasma membrane proteins in fact localizes to endocytic structures supports the idea that the secretory and endocytic pathways intersect (Futter et al., 1995; Harsay and Schekman, 2002). Because recycling endosomes in MDCK cells may be associated with polarized sorting during endocytosis (Hedman et al., 1987; Stoorvogel et al., 1988; Sheff et al., 1999), an intersection at this level would provide a common intracellular site at which polarity is generated. Although additional work will be required to establish this point functionally, our current experiments suggest a number of testable hypotheses.

The final issue raised concerns the mechanism of Rab8 action. The missorting phenotype was observed upon expression of a constitutively active Rab8 GTPase allele or overexpression of wild-type Rab8. No effect was observed when a dominant-negative Rab8 allele was expressed. Conceivably, the dominant-negative allele was simply inactive, as opposed to acting in a dominant-negative fashion. If true, only the active allele would be expected to interfere with the normal cycle of nucleotide binding and hydrolysis, perhaps by sequestering one or more Rab8 effectors. Such a mechanism might interfere with the proper sorting of AP-1B cargo into forming transport vesicles or might block transport vesicle formation itself. In turn, this would be expected to cause VSV-G to "leak," at least in part, into the apical pathway, as is seen for other basolateral proteins when the AP-1B pathway is not available. Alternatively, active Rab8 might somehow enhance the apical pathway itself, rendering apical missorting of proteins with basolateral targeting signals quantitatively more efficient. Finally, as is possible in the case of Cdc42, Rab8 may affect sorting or traffic via the actin cytoskeleton. Rab8 is similar to Rho family GTPases by the fact that its hypervariable domain contains only a single prenyl group (Joberty et al., 1993). Moreover, when greatly overexpressed, active Rab8 will cause the formation of dendritic extensions in neurons and even MDCK cells (although not under the conditions used here; Peranen et al., 1996). In any event, we suspect that a search for Rab8-interacting proteins, as has been accomplished for other Rab proteins, will yield important insights not only into Rab8 function in particular, but polarized sorting in general.

Materials and methods

Plasmid construction

Wild-type and mutant Rab8 cDNA were obtained from Johan Peranen (University of Helsinki, Helsinki, Finland; Peranen et al., 1996). T7-tagged Rab8 mutants were PCRed using primers 5′-CGGGATCCATGGCTAGCATGACTGGTGGACAGCAAATGGGTGAAGACCTACGATTACCT-3′ and 5′-GTCAAGCTTCACAGAAGAACACATCGG-3′ into BamHI–HindIII sites of pRK5. EGFP-tagged Rab8 was made by ligating Rab8 to the EcoRI site of EGFP-C1 using 5′-GCGAATTCTGCGAAGACCTACGATTACCT-3′ (EcoRI-Rab8) and 5′-CCGATGTGTTCTTCTGTGACTCTAGAG-3′ (Rab8-XbaI; the reverse primer for Rab8Q67L was 5′-CCGCTCGAGTCACAGAAGAACACATCGGAA-3′). EGFP-Rab8 was cloned into pAdEasy™ shuttle

vector at KpnI–XbaI or KpnI–XhoI (for Rab8Q67L) using primers 5′-GGGGTACCATGGTGAGCAAGGGCGAGGAGCTG-3′ (KpnI-EGFP) and 5′-CTCTAGTCACAGAAGAACACATCGG-3′ (Rab8-XbaI) or 5′-CCGCTCGAGTCACAGAAGAACACATCGGAA-3′ (Rab8-XhoI). Nonprenylated Rab8 (Rab8ΔC) was made using the forward T7 or EGFP Rab8 primers with 5′-GCTCTAGATCATCGGAAAAAGCTGCTCCTCTT-3′ cloned into shuttle vector using KpnI–XbaI sites.

Recombinant adenovirus construction

T7-tagged Rab8 was cloned into pAdEasy™ shuttle vector at KpnI–XhoI using primers 5′-GGGGTACCATGGCTAGCATGACTGGTGGACAGCAAATGGGTGCGAAGACCTACGATTACCTG-3′ and 5′-CCGCTCGAGTCACAGAAGAACACATCGGAA-3′. Rab8ΔC used primer 5′-CCCAAGCTTTCATCGGAAAAAGCTGCTCCTCTT-3′. Shuttle vector constructs were recombined with pAdEasy™-1 vector as described in the Qbiogene manual, version 1.3.

Cell culture

MDCK cells were cultured in MEM (10% FBS) and plated on clear permeable Transwell polycarbonate filters (Corning Costar) at 10^5 cells/cm^2. Cells were grown 4 d and microinjected in Hepes-buffered media after excision from filter holders. The cDNA for Rab8, LDLR, and VSV-G–GFP cDNAs (0.2 mg/ml) were injected into nuclei of ~400 cells using an Eppendorf Transjector microinjection system mounted on an inverted microscope (Axiovert; Carl Zeiss MicroImaging, Inc.) with a 40°C heated stage. After injection, the filters were incubated at 40°C for 2 h for ts045 VSV-G GFP expression and for retention in the ER. Cells injected with LDLR or FcR were incubated at 37°C for 1 h, at 20°C for 2–2.5 h, and then returned to 37°C for 2 h with 0.1 mg/ml cycloheximide. Filters were fixed in 4% PFA and processed for IF. LLC-PK1 cells were cultured in α-MEM, 10% FBS, and 1.8 mg/ml geneticin. μ1A−/μ1B+ fibroblasts (Eskelinen et al., 2002) were grown in Dulbecco's minimum essential medium (DMEM), 10% FBS, and 200 μg/ml hygromycin. For IF, cells were seeded on Alcian blue–coated coverslips and cultured for 3 d before transfection. MDCK-Tfn receptor (MDCKT) stable cells were cultured in DMEM, 10% FBS, and 0.5 g/ml geneticin as described previously (Sheff et al., 1999.)

Recombinant adenoviruses and transfection

The ts045 VSV-G–GFP and apical variant were gifts from Patrick Keller (European Molecular Biology Laboratory, Heidelberg, Germany; Keller et al., 2001). Cells were infected 24 h before analysis by IF or pulse-chase biotinylation. Cells were infected at 4 plaque-forming units/cell. Propagation and generation of recombinant adenoviruses were performed as described in the pAdEasy™ vector protocol (Qbiogene). LipofectAMINE™ (Invitrogen) was used for transient transfection in LLC-PK1 and embryonic fibroblast cells.

IF microscopy

For total cell staining, cells were fixed in 4% PFA for 15 min followed by 5–10 min of blocking/permeabilization in PBS with 10% goat serum (GS) and 0.25% saponin. Cells were incubated for 1 h with primary antibody diluted in blocking solution (BS). The cells were washed three times for 10 min and incubated for 30 min in secondary antibody (with appropriate Alexa® Fluors; (Molecular Probes, Inc.). The cells were washed three times for 10 min in PBS and mounted in Mowiol/DABCO/glycerol solution. For surface staining, after fixation, cells were blocked in 10% GS before labeling with the first primary antibody for 1 h. Cells were then washed three times for 10 min in BS. The cells were incubated in BS plus saponin for labeling with a second primary antibody or followed with secondary antibody. If another primary antibody was used, the cells were processed as above for total cell staining.

Confocal microscopy was performed using a laser scanning microscope (LSM 510; Carl Zeiss MicroImaging, Inc.), 40× water immersion lens (n = 1.5), at 25°C. Images were processed using Adobe Photoshop® (Adobe Systems, Inc.) version 7.0 software and Volocity (Improvision) version 2.0.1 software.

Antibodies

Antibodies used are as follows: C7, a mouse mAb to LDLR ectodomain (American Type Culture Collection); anti-T7, mouse mAb to T7 tag (Novagen); anti-cis Golgi, GM130 (Martin Lowe, University of Manchester, Manchester, UK); anti-Golgi, giantin (David Shima, Imperial Cancer Research Fund, London, UK), furin (Affinity BioReagents, Inc.); anti-γ-adaptin were rabbit polyclonal (Margaret Robinson, University of Cambridge, Cambridge, UK); mouse monoclonal clone 88 (Transduction Labs); and clone 100/3 (Sigma-Aldrich). Anti-VSV-G, for IF, TK-G (Thomas Kreis), and for immunoprecipitation P5D4 (Thomas Kreis).

Pulse-chase biotinylation

Pulse-chase assays were performed as described previously (Matter et al., 1992). Samples were immunoprecipitated using P5D4 coupled to protein G–Sepharose beads (Zymed Laboratories). Biotinylated surface proteins were pulled down using neutravidin beads (Pierce Chemical Co.). Samples were analyzed by SDS-PAGE followed by Western blot. The gels were dried and quantitative autoradiography was performed using a PhosphorImager (Storm 860; Molecular Dynamics).

FACS® analysis

Flow cytometry was performed with a FACSCalibur™ with CellQuest software (Becton Dickinson) for acquisition and with FlowJo (TreeStar) for analysis. Secondary antibodies were anti–mouse phytoerythrin (Sigma-Aldrich).

Tfn uptake

MDCKT cells grown on coverslips and induced with 10 mM butyrate for 14 h. Cells were preincubated in serum-free media for 30 min at 37°C. Coverslips were inverted on a droplet of 100 μg/ml Tfn 594 or Tfn 488 (Molecular Probes, Inc.) in PBS on ice for 30 min, followed by incubation at 37°C for 22 min. Cells were processed for IF as described above.

Immuno-EM

EM was performed as described previously (Fölsch et al., 2001) using anti-GFP (CLONTECH Laboratories, Inc.) and anti-Alexa® 488 (Molecular Probes, Inc.).

We would like to thank J. Peranen for the Rab8 constructs, P. Keller for the VSV-G adenoviruses, and M.S. Robinson for the rabbit polyclonal γ-adaptin antibody. Many thanks to G. Warren, H. Chang, E. Anderson, S. Maday, and D. Sheff for helpful discussions and comments; J. Lee for expert assistance; and to the entire Mellman/Warren laboratory for their enthusiastic support.

This work was supported by the National Institutes of Health (grants GM29765 and CA46128 to I. Mellman) and by the Ludwig Institute for Cancer Research.

Submitted: 8 July 2003
Accepted: 11 September 2003

References

Aroeti, B., and K.E. Mostov. 1994. Polarized sorting of the polymeric immunoglobulin receptor in the exocytotic and endocytotic pathways is controlled by the same amino acids. *EMBO J.* 13:2297–2304.

Carroll, K.S., J. Hanna, I. Simon, J. Krise, P. Barbero, and S.R. Pfeffer. 2001. Role of Rab9 GTPase in facilitating receptor recruitment by TIP47. *Science.* 292: 1373–1376.

Cohen, D., A. Musch, and E. Rodriguez-Boulan. 2001. Selective control of basolateral membrane protein polarity by cdc42. *Traffic.* 2:556–564.

Drubin, D.G., and W.J. Nelson. 1996. Origins of cell polarity. *Cell.* 84:335–344.

Erickson, J.W., C. Zhang, R.A. Kahn, T. Evans, and R.A. Cerione. 1996. Mammalian Cdc42 is a brefeldin A-sensitive component of the Golgi apparatus. *J. Biol. Chem.* 271:26850–26854.

Eskelinen, E.L., C. Meyer, H. Ohno, K. von Figura, and P. Schu. 2002. The polarized epithelia-specific mu 1B-adaptin complements mu 1A-deficiency in fibroblasts. *EMBO Rep.* 3:471–477.

Fölsch, H., H. Ohno, J.S. Bonifacino, and I. Mellman. 1999. A novel clathrin adaptor complex mediates basolateral targeting in polarized epithelial cells. *Cell.* 99:189–198.

Fölsch, H., M. Pypaert, P. Schu, and I. Mellman. 2001. Distribution and function of AP-1 clathrin adaptor complexes in polarized epithelial cells. *J. Cell Biol.* 152:595–606.

Fölsch, H., M. Pypaert, S. Maday, L. Pelletier, and I. Mellman. 2003. The AP-1A and AP-1B adaptor complexes define biochemically and functionally distinct membrane domains. *J. Cell Biol.* 163:351–362.

Futter, C.E., C.N. Connolly, D.F. Cutler, and C.R. Hopkins. 1995. Newly synthesized transferrin receptors can be detected in the endosome before they appear on the cell surface. *J. Biol. Chem.* 270:10999–11003.

Gan, Y., T.E. McGraw, and E. Rodriguez-Boulan. 2002. The epithelial-specific adaptor AP1B mediates post-endocytic recycling to the basolateral mem-

brane. *Nat. Cell Biol.* 4:605–609.

Grindstaff, K.K., C. Yeaman, N. Anandasabapathy, S.C. Hsu, E. Rodriguez-Boulan, R.H. Scheller, and W.J. Nelson. 1998. Sec6/8 complex is recruited to cell-cell contacts and specifies transport vesicle delivery to the basal-lateral membrane in epithelial cells. *Cell.* 93:731–740.

Guo, W., D. Roth, E. Gatti, P. De Camilli, and P. Novick. 1997. Identification and characterization of homologues of the Exocyst component Sec10p. *FEBS Lett.* 404:135–139.

Guo, W., D. Roth, C. Walch-Solimena, and P. Novick. 1999. The exocyst is an effector for Sec4p, targeting secretory vesicles to sites of exocytosis. *EMBO J.* 18:1071–1080.

Harsay, E., and R. Schekman. 2002. A subset of yeast vacuolar protein sorting mutants is blocked in one branch of the exocytic pathway. *J. Cell Biol.* 156: 271–285.

Hedman, K., K.L. Goldenthal, A.V. Rutherford, I. Pastan, and M.C. Willingham. 1987. Comparison of the intracellular pathways of transferrin recycling and vesicular stomatitis virus membrane glycoprotein exocytosis by ultrastructural double-label cytochemistry. *J. Histochem. Cytochem.* 35:233–243.

Hirst, J., W.W. Lui, N.A. Bright, N. Totty, M.N. Seaman, and M.S. Robinson. 2000. A family of proteins with gamma-adaptin and VHS domains that facilitate trafficking between the trans-Golgi network and the vacuole/lysosome. *J. Cell Biol.* 149:67–80.

Huber, L.A., S. Pimplikar, R.G. Parton, H. Virta, M. Zerial, and K. Simons. 1993. Rab8, a small GTPase involved in vesicular traffic between the TGN and the basolateral plasma membrane. *J. Cell Biol.* 123:35–45.

Huber, L.A., P. Dupree, and C.G. Dotti. 1995. A deficiency of the small GTPase rab8 inhibits membrane traffic in developing neurons. *Mol. Cell. Biol.* 15: 918–924.

Hunziker, W., and C. Fumey. 1994. A di-leucine motif mediates endocytosis and basolateral sorting of macrophage IgG Fc receptors in MDCK cells. *EMBO J.* 13:2963–2967.

Hunziker, W., C. Harter, K. Matter, and I. Mellman. 1991. Basolateral sorting in MDCK cells requires a distinct cytoplasmic domain determinant. *Cell.* 66: 907–920.

Jareb, M., and G. Banker. 1998. The polarized sorting of membrane proteins expressed in cultured hippocampal neurons using viral vectors. *Neuron.* 20: 855–867.

Joberty, G., A. Tavitian, and A. Zahraoui. 1993. Isoprenylation of Rab proteins possessing a C-terminal CaaX motif. *FEBS Lett.* 330:323–328.

Joberty, G., C. Petersen, L. Gao, and I.G. Macara. 2000. The cell-polarity protein Par6 links Par3 and atypical protein kinase C to Cdc42. *Nat. Cell Biol.* 2:531–539.

Johnson, D.I. 1999. Cdc42: an essential Rho-type GTPase controlling eukaryotic cell polarity. *Microbiol. Mol. Biol. Rev.* 63:54–105.

Keller, P., D. Toomre, E. Diaz, J. White, and K. Simons. 2001. Multicolour imaging of post-Golgi sorting and trafficking in live cells. *Nat. Cell Biol.* 3:140–149.

Koivisto, U.M., A.L. Hubbard, and I. Mellman. 2001. A novel cellular phenotype for familial hypercholesterolemia due to a defect in polarized targeting of LDL receptor. *Cell.* 105:575–585.

Kroschewski, R., A. Hall, and I. Mellman. 1999. Cdc42 controls secretory and endocytic transport to the basolateral plasma membrane of MDCK cells. *Nat. Cell Biol.* 1:8–13.

Matter, K., and I. Mellman. 1994. Mechanisms of cell polarity: sorting and transport in epithelial cells. *Curr. Opin. Cell Biol.* 6:545–554.

Matter, K., W. Hunziker, and I. Mellman. 1992. Basolateral sorting of LDL receptor in MDCK cells: the cytoplasmic domain contains two tyrosine-dependent targeting determinants. *Cell.* 71:741–753.

Matter, K., J.A. Whitney, E.M. Yamamoto, and I. Mellman. 1993. Common signals control low density lipoprotein receptor sorting in endosomes and the Golgi complex of MDCK cells. *Cell.* 74:1053–1064.

Matter, K., E.M. Yamamoto, and I. Mellman. 1994. Structural requirements and sequence motifs for polarized sorting and endocytosis of LDL and Fc receptors in MDCK cells. *J. Cell Biol.* 126:991–1004.

Mellman, I. 1996. Endocytosis and molecular sorting. *Annu. Rev. Cell. Dev. Biol.* 12:575–625.

Meyer, C., D. Zizioli, S. Lausmann, E.L. Eskelinen, J. Hamann, P. Saftig, K. von Figura, and P. Schu. 2000. mu1A-adaptin-deficient mice: lethality, loss of AP-1 binding and rerouting of mannose 6-phosphate receptors. *EMBO J.* 19:2193–2203.

Moritz, O.L., B.M. Tam, L.L. Hurd, J. Peranen, D. Deretic, and D.S. Papermaster. 2001. Mutant rab8 impairs docking and fusion of rhodopsin-bearing post-Golgi membranes and causes cell death of transgenic *Xenopus* rods. *Mol. Biol. Cell.* 12:2341–2351.

Moskalenko, S., D.O. Henry, C. Rosse, G. Mirey, J.H. Camonis, and M.A. White. 2002. The exocyst is a Ral effector complex. *Nat. Cell Biol.* 4:66–72.

Mostov, K.E., M. Verges, and Y. Altschuler. 2000. Membrane traffic in polarized epithelial cells. *Curr. Opin. Cell Biol.* 12:483–490.

Musch, A., D. Cohen, G. Kreitzer, and E. Rodriguez-Boulan. 2001. cdc42 regulates the exit of apical and basolateral proteins from the trans-Golgi network. *EMBO J.* 20:2171–2179.

Nelson, W.J. 2003. Adaptation of core mechanisms to generate cell polarity. *Nature.* 422:766–774.

Odorizzi, G., A. Pearse, D. Domingo, I.S. Trowbridge, and C.R. Hopkins. 1996. Apical and basolateral endosomes of MDCK cells are interconnected and contain a polarized sorting mechanism. *J. Cell Biol.* 135:139–152.

Ohno, H., R.C. Aguilar, D. Yeh, D. Taura, T. Saito, and J.S. Bonifacino. 1998. The medium subunits of adaptor complexes recognize distinct but overlapping sets of tyrosine-based sorting signals. *J. Biol. Chem.* 273:25915–25921.

Ohno, H., T. Tomemori, F. Nakatsu, Y. Okazaki, R.C. Aguilar, H. Foelsch, I. Mellman, T. Saito, T. Shirasawa, and J.S. Bonifacino. 1999. Mu1B, a novel adaptor medium chain expressed in polarized epithelial cells. *FEBS Lett.* 449:215–220.

Peranen, J., and J. Furuhjelm. 2001. Expression, purification, and properties of Rab8 function in actin cortical skeleton organization and polarized transport. *Methods Enzymol.* 329:188–196.

Peranen, J., P. Auvinen, H. Virta, R. Wepf, and K. Simons. 1996. Rab8 promotes polarized membrane transport through reorganization of actin and microtubules in fibroblasts. *J. Cell Biol.* 135:153–167.

Puertollano, R., R.C. Aguilar, I. Gorshkova, R.J. Crouch, and J.S. Bonifacino. 2001. Sorting of mannose 6-phosphate receptors mediated by the GGAs. *Science.* 292:1712–1716.

Roush, D.L., C.J. Gottardi, H.Y. Naim, M.G. Roth, and M.J. Caplan. 1998. Tyrosine-based membrane protein sorting signals are differentially interpreted by polarized Madin-Darby canine kidney and LLC-PK1 epithelial cells. *J. Biol. Chem.* 273:26862–26869.

Sheff, D.R., E.A. Daro, M. Hull, and I. Mellman. 1999. The receptor recycling pathway contains two distinct populations of early endosomes with different sorting functions. *J. Cell Biol.* 145:123–139.

Stoorvogel, W., H.J. Geuze, J.M. Griffith, and G.J. Strous. 1988. The pathways of endocytosed transferrin and secretory protein are connected in the trans-Golgi reticulum. *J. Cell Biol.* 106:1821–1829.

Sugimoto, H., M. Sugahara, H. Fölsch, Y. Koide, F. Nakatsu, N. Tanaka, T. Nishimura, M. Furukawa, C. Mullins, N. Nakamura, et al. 2002. Differential recognition of tyrosine-based basolateral signals by AP-1B subunit micro1B in polarized epithelial cells. *Mol. Biol. Cell.* 13:2374–2382.

TerBush, D.R., T. Maurice, D. Roth, and P. Novick. 1996. The Exocyst is a multiprotein complex required for exocytosis in *Saccharomyces cerevisiae*. *EMBO J.* 15:6483–6494.

Teuchert, M., W. Schafer, S. Berghofer, B. Hoflack, H.D. Klenk, and W. Garten. 1999. Sorting of furin at the trans-Golgi network. Interaction of the cytoplasmic tail sorting signals with AP-1 Golgi-specific assembly proteins. *J. Biol. Chem.* 274:8199–8207.

Thomas, D.C., and M.G. Roth. 1994. The basolateral targeting signal in the cytoplasmic domain of glycoprotein G from vesicular stomatitis virus resembles a variety of intracellular targeting motifs related by primary sequence but having diverse targeting activities. *J. Biol. Chem.* 269:15732–15739.

Yeaman, C., K.K. Grindstaff, J.R. Wright, and W.J. Nelson. 2001. Sec6/8 complexes on trans-Golgi network and plasma membrane regulate late stages of exocytosis in mammalian cells. *J. Cell Biol.* 155:593–604.

Zhang, X., E. Bi, P. Novick, L. Du, K.G. Kozminski, J.H. Lipschutz, and W. Guo. 2001. Cdc42 interacts with the exocyst and regulates polarized secretion. *J. Biol. Chem.* 276:46745–46750.

Zizioli, D., C. Meyer, G. Guhde, P. Saftig, K. von Figura, and P. Schu. 1999. Early embryonic death of mice deficient in gamma-adaptin. *J. Biol. Chem.* 274:5385–5390.